Natural Resources Canada
Ressources naturelles Canada

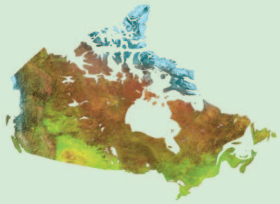

Petrological investigation of ultramafic-mafic plutonic rocks, Southampton Island, Nunavut

Peterson, T.D., Sanborn-Barrie, M., and Chakungal, J.

Geological Survey of Canada

Current Research 2011-15

2011

Canada

Geological Survey of Canada
Current Research 2011-15

Petrological investigation of ultramafic-mafic plutonic rocks, Southampton Island, Nunavut

Peterson, T.D., Sanborn-Barrie, M., and Chakungal, J.

2011

ISSN 1701-4387
Catalogue No. M44-2011/15E-PDF
ISBN 978-1-100-19309-0
doi: 10.4095/289244

A copy of this publication is also available for reference in depository libraries across Canada through access to the Depository Services Program's Web site at http://dsp-psd.pwgsc.gc.ca

A free digital download of this publication is available from GeoPub: http://geopub.nrcan.gc.ca/index_e.php

Toll-free (Canada and U.S.A.): 1-888-252-4301

Recommended citation

Peterson, T.D., Sanborn-Barrie, M., and Chakungal, J., 2011. Petrological investigation of ultramafic-mafic plutonic rocks, Southampton Island, Nunavut; Geological Survey of Canada, Current Research 2011-15, 11 p. doi:10.4095/289244

Critical review

J. Whalen

Authors

T.D. Peterson (Tony.Peterson@NRCan-RNCan.gc.ca)
M. Sanborn-Barrie (Mary.Sanborn-Barrie@NRCan-RNCan.gc.ca)
Geological Survey of Canada
601 Booth Street
Ottawa, Ontario
K1A 0E9

J. Chakungal (joyia.chakungal@gmail.com)
formerly at Canada–Nunavut Geoscience Office
Iqaluit, Nunavut
X0A 0H0

Correction date:

Petrological investigation of ultramafic-mafic plutonic rocks, Southampton Island, Nunavut

Peterson, T.D., Sanborn-Barrie, M., and Chakungal, J.

Peterson, T.D., Sanborn-Barrie, M., and Chakungal, J., 2011. Petrological investigation of ultramafic-mafic plutonic rocks, Southampton Island, Nunavut; Geological Survey of Canada, Current Research 2011-15, 11 p. doi:10.4095/289244

Abstract: Selected outcrops of Paleoproterozoic ultramafic intrusive rocks on Southampton Island are characterized by their mineralogy as having tholeiitic parental magmas. Clino- and orthoamphiboles partially replacing pyroxenes are interpreted as products of subsolidus hydration. Chromite phenocrysts have less than 10% MgO and less than 33% Cr_2O_3 and are, accordingly, distinct from kimberlitic spinels also found on the island. Isotopic data and the occasional presence of phlogopite indicate that the magmas interacted with granitic wall rock, such that the geochemistry of the samples is not a completely reliable indicator of provenance. There is no evidence of primary magmatic concentration of PGEs, but secondary (hydrothermal) concentration together with As and Sb is indicated.

Résumé : Dans l'île Southampton, certains affleurements de roches intrusives ultramafiques du Paléoprotérozoïque sont caractérisés par leur minéralogie comme étant issus de magmas parentaux tholéiitiques. Des clinoamphiboles et des orthoamphiboles qui remplacent partiellement des pyroxènes sont interprétées comme étant des produits d'une hydratation subsolidus. Des phénocristaux de chromite ont une teneur inférieure à 10 % en MgO et inférieure à 33 % en Cr_2O_3, ce qui les distingue des spinelles kimberlitiques également présents dans l'île. Des données isotopiques et la présence occasionnelle de phlogopite indiquent qu'il y a eu une interaction entre les magmas et la roche granitique encaissante, de sorte que la géochimie des échantillons n'est pas un indicateur totalement fiable de la provenance. Il n'y a aucune preuve de concentration primaire des éléments du groupe du platine (ÉGP) dans le magma, mais une concentration secondaire (hydrothermale) avec As et Sb est indiquée.

INTRODUCTION

Recent geological mapping (1:150 000) of Southampton Island, Nunavut, has resulted in identification of approximately 100 isolated exposures of peridotite and pyroxenite, 50 to 500 m wide, mainly distributed throughout the Precambrian highland exposed on the eastern half of the island (Chakungal et al., 2007; Sanborn-Barrie et al., 2008a). In some instances, these rocks preserve macroscopic primary igneous features. Some of the larger outcrops contain horizons of gabbro and gabbroic anorthosite. Many of the peridotitic samples contain significant amounts of chromite, which is a prominent detrital mineral found in the Quaternary deposits of the area (Ross and Kosar, 2009).

Uranium-lead dating indicates at least three mafic-ultramafic plutonic events are recorded on Southampton Island (Rayner et al., 2011). There is a pre-1930 Ma granulite mafic complex cut and hydrated by quartz porphyry (sample 07CYA-M98) of that age; a 1870 ± 10 Ma layered ultramafic-mafic complex dated by gabbroic anorthosite (sample 07CYA-M38b); and a 1842 ± 5 Ma diorite complex (sample 07CYA-M133a). Unpublished isotopic data from additional mafic plutons further support ultramafic-mafic events at ca. 2.05 Ga and ca. 1.88 Ga (N. Rayner, unpub. data, 2009), highlighting the episodic nature of ultramafic-mafic magmatic activity in this region during the Paleoproterozoic.

Detailed study of Southampton Island's mafic-ultramafic plutonic rocks was undertaken in order to provide a context for better understanding potential Ni-Cu-PGEs in this underexplored region of Nunavut. Although the mapped exposures may be too small to be of economic interest, they may indicate potential for chromite-rich, platinum group element (PGE)–bearing rocks at depth below the exposed Archean, and/or beneath Phanerozoic cover on the western side of the island. Study of these plutonic rocks may also provide insight into the nature of their parental magma from which correlation with rocks having similar lithologies may be based, and clues to the Precambrian tectonic evolution of the region.

A subset of the largest and most pristine ultramafic intrusions located across the island (Fig. 1a) was selected for this study (for a detailed geological map *see* Sanborn-Barrie et al., 2008a). In outcrop, smaller exposures of ultramafic material

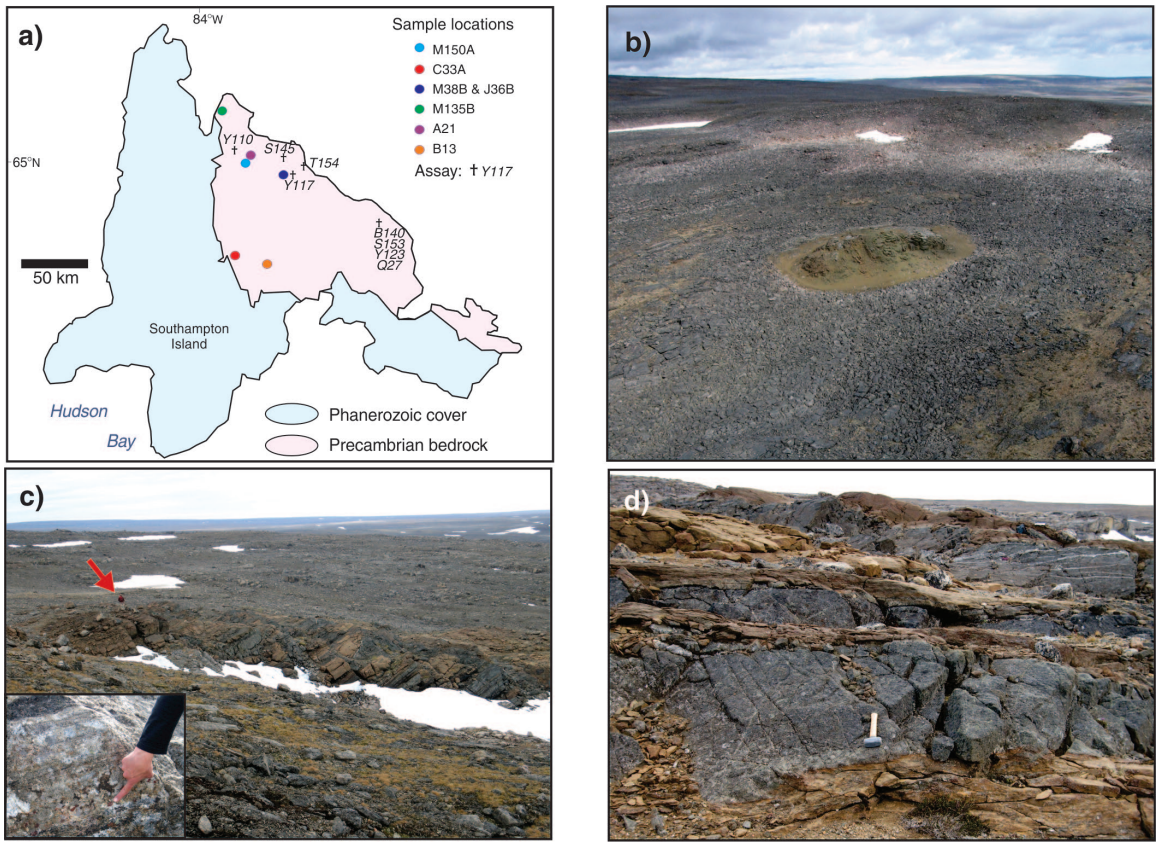

Figure 1. Selected ultramafic intrusive rocks of Southampton Island, Nunavut. **a)** Locations of samples described in this study. **b)** Aerial view of peridotitic outcrop (station 07CYA-M150a), approximately 200 m across. 2010–177. **c)** Kokumiak River layered plutonic complex (site of samples M38B and J36B) comprising moderately dipping alternating peridotite and pyroxenite with minor gabbroic anorthosite (inset) dated at 1870 ± 10 Ma (Rayner et al., 2011). Geologist indicated by red arrow for scale. 2010–178. **d)** Closer view of Kokumiak River layered plutonic complex showing orange-brown-weathered peridotite alternating with dark grey-green pyroxenite. Hammer, 300 cm long, for scale. 2010–179. Photographs by M. Sanborn-Barrie.

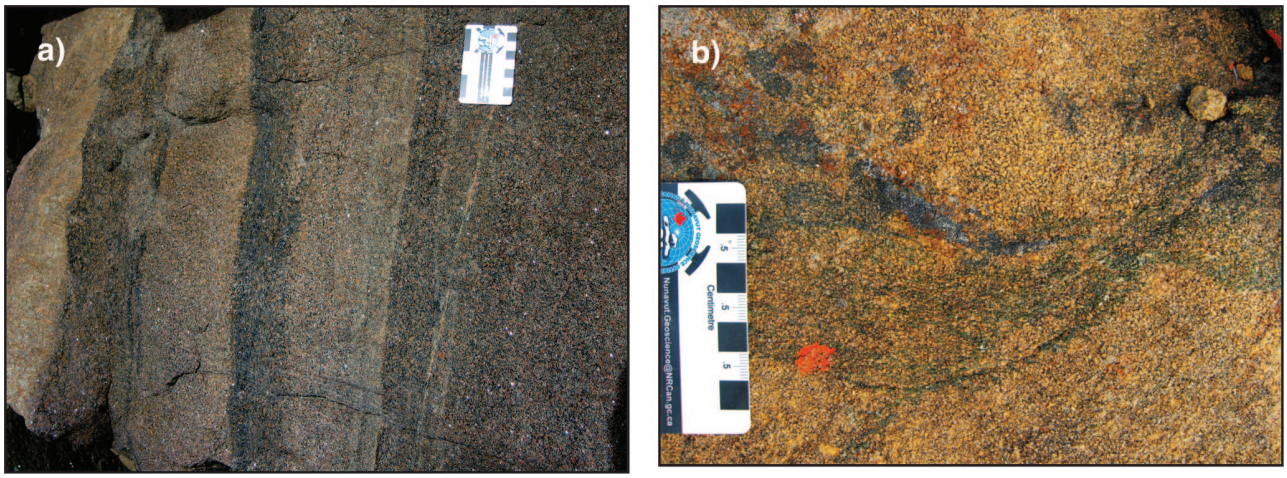

Figure 2. Primary magmatic features in ultramafic rocks, Southampton Island. **a)** Centimetre-scale modal layering with compositional variations consistent with top to the right. 2010–080. **b)** Chromite-rich layers in peridotite, station C33. The appearance of these dark, thin layers suggests initial magmatic settling in an intrusion, followed by extension and slumping of a crystal mush along a top right to bottom left slip surface. GSC photo 2010–181. Photographs by M. Sanborn-Barrie.

are typically lenticular (e.g. Fig. 1b) and tabular, or sill-like. The margins of these bodies are usually fine grained, with mineralogy similar to their coarser grained interiors. Locally, a rind of hydrous minerals occurs at the interface between the ultramafic rocks and adjacent wall rocks. The largest of the intrusions (the site of samples J36B and M38b), dated at 1870 ± 10 Ma (Rayner et al., 2011), display tectonically modified igneous layering (Fig. 1c, d) with metre-scale differentiation of peridotite, pyroxenite, and gabbroic anorthosite (Fig. 1c inset). This intrusive complex is informally designated the Kokumiak River layered plutonic complex, given its location south of the headwaters of a major river that flows east to Kokumiak Harbour. Rocks at other localities display centimetre-scale magmatic layering (Fig. 2a) and/or features indicative of crystal sedimentation and slumping of layers (Fig. 2b).

With the exception of the Kokumiak River layered plutonic complex, which is hosted by foliated to gneissic charnockitic wall rocks, tabular or sill-like mafic plutonic occurrences are often associated with metasedimentary rocks. An intrusive relationship between mafic/ultramafic rocks and metasedimentary rocks is obscured by the parallel concordant nature of these typically high-strain contacts, but is inferred on the basis of the close spatial association of these two lithologies. Composite metasedimentary–ultramafic/mafic plutonic enclaves are wrapped by orthogneiss, and are interpreted to represent boudins of once more coherent bodies pulled apart during subsequent regional deformation. Alternatively, some ultramafic exposures (e.g. Fig. 1b) may represent ultramafic plugs that were emplaced into the orthogneissic basement complex at a relatively late stage of regional deformation.

MINERALOGY

Sample descriptions

The samples for this study (Fig. 1a) were selected on the basis of minimal alteration, and/or mineralogical diversity. Polished thin sections were studied optically and by scanning electron microscope (SEM), followed by mineral analyses with an electron microprobe. Specific descriptions below are given in the order of least evolved (peridotites) to most evolved (feldspathic pyroxenite), as determined by petrography and mineral compositions.

Sample 07CYA - C33A

This sample is dominated by olivine, with variable amounts of orthopyroxene (up to 30%) and clinopyroxene (up to 15%), and approximately 5% chromite (Fig. 3). Weak primary layering in the form of centimetre-scale bands of chromite (Fig. 2) is present, but a penetrative deformational fabric is absent. Silicate minerals have an average grain size of ~2 mm. Clinopyroxene is colourless in thin section, while orthopyroxene is a very pale brown. Both pyroxenes are free of inclusions and lack exsolution features. Although a majority of orthopyroxene grains are anhedral, a small number (~10%) are subidiomorphic and partially bounded by flat faces. Silicate minerals may be transected by a fine network of serpentine-filled fractures.

Sample 07CYA - M150A

This sample is a fine grained (~0.25 mm) peridotite, with near-equal amounts of olivine, orthopyroxene, and clinopyroxene, and ~5% very fine-grained (0.1 mm) chromite (Fig. 4).

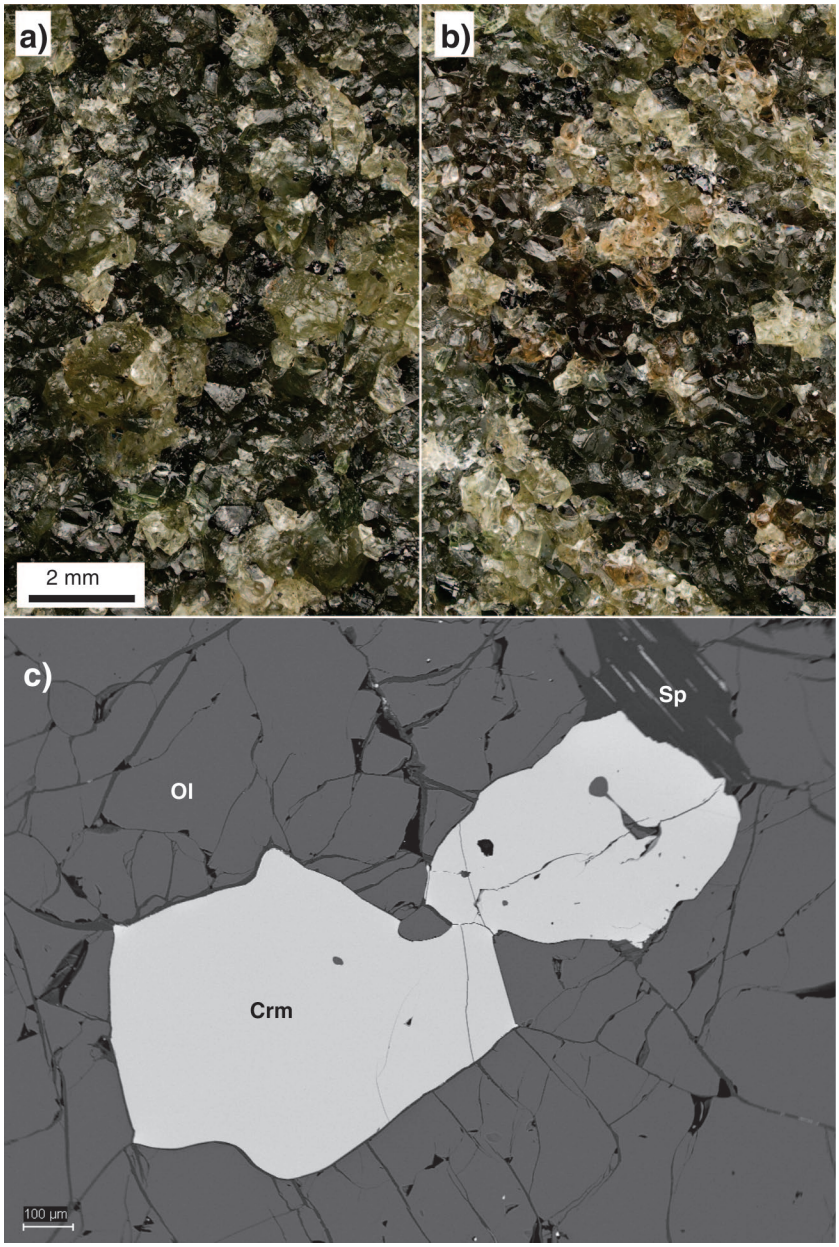

Figure 3. Relatively coarse-grained peridotite C33A. **a)** Freshly broken surface dominated by olivine with minor chromite (black) and clinopyroxene (grass-green). 2010–182. **b)** Another area of sample C33A, showing minor brown orthopyroxene. 2010–183. **c)** SEM image of a polished section of sample C33A, showing the anhedral form of chromite (Crm) and olivine (Ol). The dark area showing cleavage is a rare grain of serpentine (Sp). 2010–184.

Figure 4. Relatively fine-grained peridotite M150 whose fresh surface exhibits abundant orthopyroxene and thin dark layers rich in olivine and chromite. 2011-184

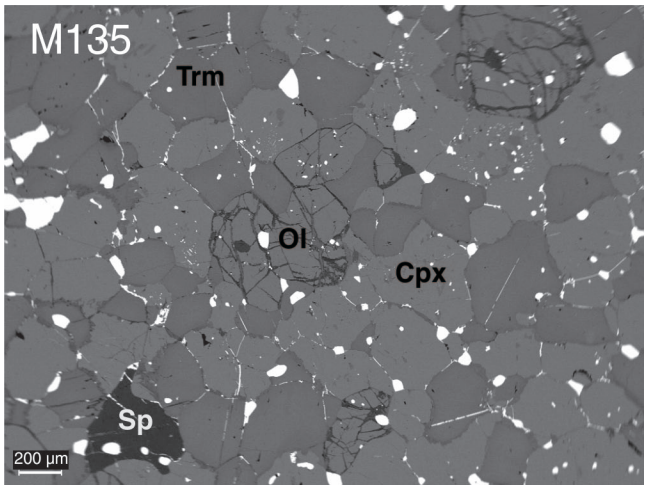

Figure 5. Backscattered electron image of a polished section of sample M135b showing silicate minerals (Ol = olivine, Cpx = clinopyroxene, Trm = tremolite-rich clinoamphibole, Sp = serpentine) in grey tones and oxides (magnetite) in white. Clinoamphibole typically displays ragged fringes, ~20 microns wide, that extend into adjacent clinopyroxene grains it has partially replaced. 2011-183

Unlike sample C33A, pyroxenes in this sample are distinct in thin section, with clinopyroxene appearing pale green and orthopyroxene displaying very pale grey-brown hues. Orthopyroxene grains typically have Mg- and Al-rich compositions. They typically contain abundant small, subhedral to euhedral chromite inclusions that are transparent on thin edges, and may contain oriented, rod-like inclusions of exsolved clinopyroxene. Secondary hydrous minerals are not present.

Sample 07CYA - J36B

This sample of coarse-grained (up to 3 mm) pyroxenite contains roughly equal amounts of orthopyroxene and clinopyroxene, ~10% olivine, and minor interstitial phlogopite that is partially chloritized. In thin-section, clinopyroxene is pale green and orthopyroxene is distinctly pleochroic from pale brown to brown-pink. Trace amounts of oriented, oxidized exsolution lamellae are typically observed in orthopyroxene and rarely in clinopyroxene. Primary and metamorphic fabrics are not distinguishable in thin section. All phases are anhedral, and magnetite is particularly well rounded.

Sample 07CYA - M135B

This sample is a fine-grained (average 0.2–0.5 mm) rock that is dominated by near-equal amounts of colourless clinopyroxene and green clinoamphibole, ~5% olivine (~25% converted to serpentine), 1% orthopyroxene, and 5% magnetite (Fig. 5). Olivine and orthopyroxene are euhedral to rounded, clinopyroxene and amphibole are subhedral, and magnetite is highly rounded and irregular. The contacts between amphibole and clinopyroxene are typically marked by a thin zone of colourless clinopyroxene(?) that is optically continuous with the amphibole. Blebs of magnetite and opaque lamellae are common as inclusions in clinopyroxene.

Sample 07CYA - A21

This sample is a phlogopite pyroxenite dominated by subhedral orthopyroxene (50%) and green clinoamphibole (30%), with 15% brown, partly aligned phlogopite and 5% untwinned plagioclase feldspar. Magnetite is absent. Numerous amphibole grains contain islands of a pale green mineral with a large volume fraction of coarse lamellae, interpreted as clinopyroxene with exsolution lamellae, replaced by amphibole. No unaltered clinopyroxene was available for microprobe analysis.

Sample 07CYA - B13

Sample B13 is a phlogopite peridotite, dominated by serpentinized olivine and a large volume fraction of crosscutting serpentine veins. Phlogopite is colourless. Orthopyroxene is subordinate, whereas clinopyroxene was not observed. An opaque spinel group mineral (~15%) is present.

Mineral Compositions

Chromite and Magnetite

Spinel compositions are provided in Table 1 and summarized Figure 6. Chromium contents of spinel phases are positively correlated both with Al and with olivine content (Fig. 6a). Cr ranges from a maximum of 33% Cr_2O_3 in sample C33A to 3% Cr_2O_3 in sample J36B. Titanium is low in Cr-rich spinels and most abundant in pyroxenite M135B (Fig. 6b) with Ti contents of 2.35%.

Olivine and Pyroxenes

Olivine compositions (Table 2) range from Fo_{89} and Fo_{88} in peridotite samples M150A and C33A to Fo_{73} in M135B, which is the most evolved rock containing olivine. Pyroxene compositions, summarized in Table 3 and Figure 7, show average orthopyroxene compositions range from En_{89} in peridotite M150 to En_{68} in phlogopite peridotite A21. It should be noted that orthopyroxene is abundant in C33A, but was not identified during microprobe analysis.

All analyzed clinopyroxenes are moderately aluminous augite. In the most olivine-rich rocks, they are close to subcalcic augite in composition, but do not plot within the metastable (X_{Wo} <0.25) or pigeonite fields.

Amphiboles and Phlogopite

Amphibole and phlogopite were analyzed from two samples (Table 4). Samples A21 and M135B contain tremolite (after clinopyroxene) that is moderately aluminous with small, but significant, contents of glaucophane and gedrite molecules.

Interpretation

The anhydrous mineral assemblages and compositions of these samples are typical of tholeiitic mafic suites and extend to compositions typical of early phenocryst phases in primary melts. The Cr_2O_3 contents of even the most Mg- and Cr-rich spinels, are well below that considered typical of diamond-indicator mineral suites, allowing recognition of mafic plutonic vs. kimberlitic affinity. It should, however, be noted that Cr grains found in till on Southampton Island by Ross and Kosar (2009) were suggestive of kimberlitic affinity.

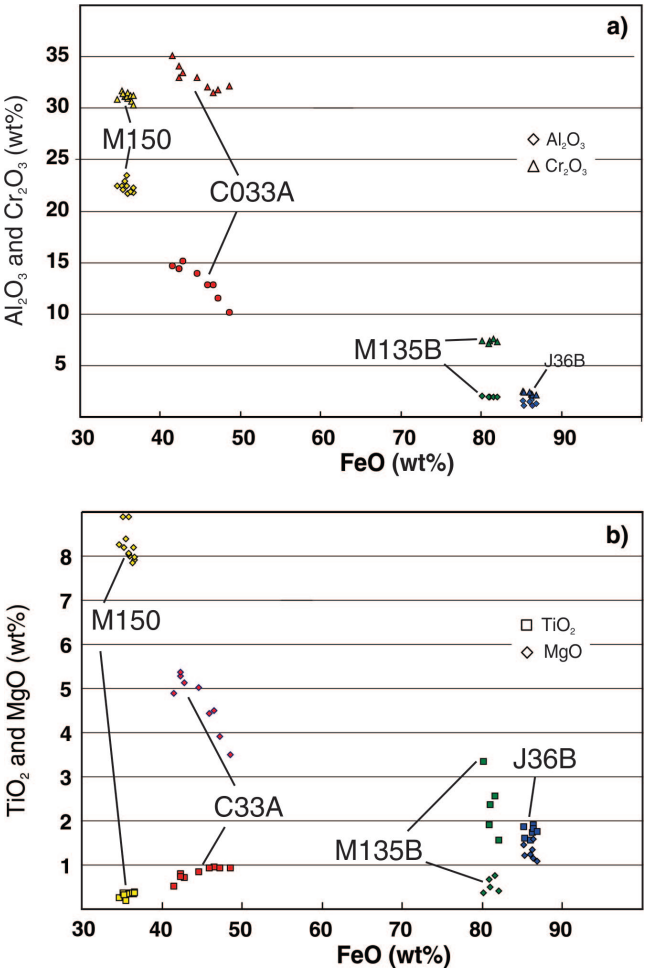

Figure 6. Compositions of spinel phases. **a)** Weight per cent Al_2O_3 and Cr_2O_3 versus FeO_{total}. **b)** Weight per cent TiO_2 and MgO versus FeO_{total}.

Table 1. Average microprobe analyses of spinel phases.

Sample	M150A	C33A	J36B	M135B
n	12	9	7	5
SiO_2	0.00	0.04	0.05	0.07
TiO_2	0.34	0.82	1.75	2.35
Al_2O_3	22.26	13.34	1.35	1.97
Cr_2O_3	31.10	32.91	2.28	7.36
V_2O_3	0.12	0.22	0.19	0.38
Nb_2O_5	0.07	0.04	0.06	0.00
FeO	35.84	44.62	86.04	81.13
MnO	0.37	0.48	0.44	0.53
MgO	8.22	4.67	1.30	0.54
NiO	0.28	0.21	0.57	0.32
ZnO	0.1	0.23	0.04	0.08
CoO	0.06	0.09	0.13	0.06
CaO	0.01	0.01	0.02	0.03
As_2O_3	0.04	0.03	0.07	0.10
SO_3	0.03	0.02	0.04	0.02
Total	**98.87**	**97.73**	**94.32**	**94.93**
Components as molecular fractions				
$MgAl_2O_4$	0.392	0.239	0.030	0.031
$MgCr_2O_4$	0.000	0.000	0.034	0.000
$MgFe_2O_4$	0.000	0.000	0.009	0.000
$FeAl_2O_4$	0.028	0.031	0.000	0.013
$FeCr_2O_4$	0.393	0.447	0.000	0.110
Fe_2TiO_4	0.008	0.021	0.050	0.067
Fe_3O_4	0.166	0.244	0.851	0.760
$Fe(V, Nb)_2O_4$	0.002	0.003	0.003	0.006
$(Ni, Co, Zn)\ Fe_2O_4$	0.011	0.014	0.022	0.014
n = number of analyses				

Table 2. Average microprobe analyses of olivine.

Sample	M150A	C33A	B13	M135B
n	6	3	2	2
SiO_2	46.20	40.81	39.45	38.53
TiO_2	0.01	0.02	0.04	0.03
Al_2O_3	0.50	0.03	0.03	0.02
$cxCr_2O_3$	0.13	0.03	0.00	0.01
V_2O_3	0.01	0.03	0.00	0.03
FeO	9.05	11.25	13.35	24.74
MnO	0.17	0.16	0.27	0.43
MgO	43.41	48.85	45.52	37.71
NiO	0.3	0.29	0.33	0.36
CaO	0.12	0.00	0.00	0.01
Na_2O	0.00	0.02	0.03	0.02
K_2O	0.00	0.01	0.03	0.00
Total	99.9	101.52	99.06	101.91
Mg/M2+	0.889	0.882	0.853	0.725
n = number of analyses				

Table 3. Average microprobe analyses of pyroxene.

Sample	M150A	M150A	C33A	J36B	J36B	M135B	M135B	A21
n	5	6	3	6	9	2	2	5
Type	cpx	opx	cpx	cpx	opx	cpx	opx	opx
SiO_2	47.14	56.6	54.34	54.50	56.16	54.70	55.37	54.21
TiO_2	0.55	0.05	0.26	0.09	0.04	0.09	0.06	0.03
Al_2O_3	10.99	1.40	4.45	1.13	1.06	0.68	0.46	0.62
Cr_2O_3	1.23	0.22	0.70	0.05	0.04	0.11	0.06	0.19
V_2O_3	0.02	0.01	0.05	0.02	0.03	0.02	0.00	0.01
FeO	4.58	7.15	3.30	3.46	10.96	4.30	15.15	18.91
MnO	0.09	0.24	0.07	0.24	0.55	0.21	0.50	0.60
MgO	18.81	33.63	22.08	17.49	31.65	17.15	28.65	25.43
NiO	0.11	0.07	0.09	0.04	0.07	0.05	0.07	0.09
CaO	13.26	0.35	12.95	24.41	0.47	24.38	0.39	0.50
Na_2O	1.81	0.01	0.50	0.04	0.01	0.17	0.00	0.01
K_2O	0.45	0.00	0.08	0.01	0.00	0.00	0.01	0.01
Total	**99.05**	**99.81**	**98.87**	**101.47**	**101.05**	**101.87**	**100.73**	**100.62**
Di	0.308	0.000	0.425	0.909	0.002	0.906	0.005	0.004
En	0.326	0.878	0.398	0.010	0.815	0.000	0.753	0.684
Fs	0.066	0.105	0.051	0.052	0.159	0.064	0.224	0.286
CaTs	0.131	0.006	0.062	0.019	0.014	0.005	0.007	0.009
Rh	0.001	0.004	0.001	0.004	0.008	0.003	0.008	0.009
Jd	0.12	0.000	0.036	0.003	0.001	0.012	0.000	0.001
CaCr	0.033	0.006	0.021	0.001	0.001	0.003	0.002	0.006
CaTi	0.014	0.001	0.007	0.002	0.001	0.002	0.002	0.001
Wo	0.000	0.000	0.000	0.000	0.000	0.005	0.000	0.000
Ac	0.000	0.000	0.000	0.000	0.000	0.000	0.000	0.000
Mg/M2+	0.880	0.894	0.923	0.900	0.837	0.877	0.771	0.706

Di = $CaMgSi_2O_6$	CaTs = $CaAl(AlSi)O_6$	CaCr = $CaCr(AlSi)O_6$
En = $Mg_2Si_2O_6$	Rh = $Mn_2Si_2O_6$	CaTi = $CaTiAl_2O_6$
Fs = $Fe_2Si_2O_6$	Jd = $NaAlSi_2O_6$	Wo = $Ca_2Si_2O_6$
		Ac = $NaFeSi_2O_6$

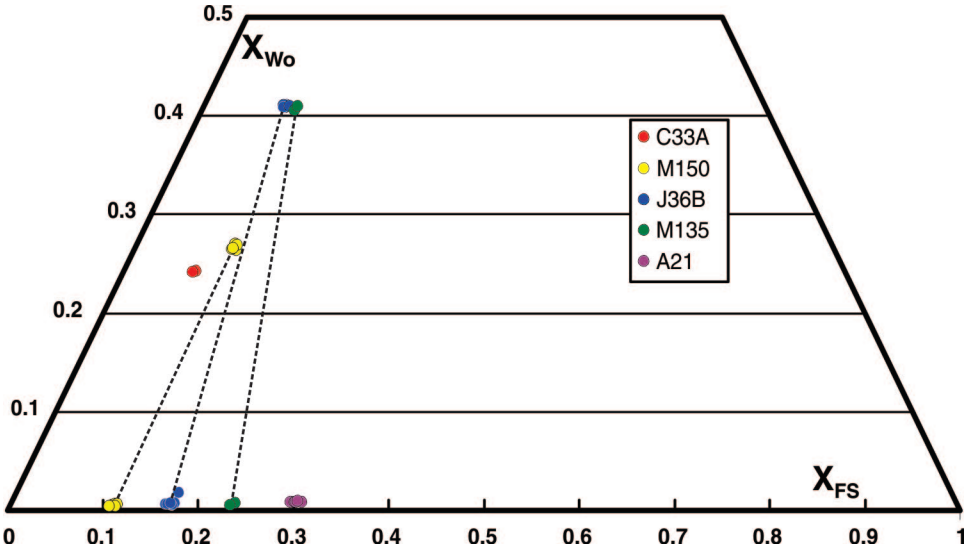

Figure 7. Compositions of pyroxenes in En-Fs-Wo, plotted as mole fraction. Tie lines join compositions of coexisting pyroxenes in one sample. Fs – ferrosilite, Wo – wollastonite.

A notable exception to tholeiitic mineral assemblages is the substantial presence of phlogopite in peridotite B13 and pyroxenite A21, and to a lesser degree in pyroxenite J36B. In all cases, phlogopite is interpreted to be a primary phenocryst phase that precipitated directly from melt. Although small amounts of phlogopite could be expected to precipitate from fractionated basalts, the volume observed in at least two of the samples, particularly the peridotite, is more consistent with assimilation of K- and H-rich granitic wall rocks. Interaction and assimilation of crustal rocks is also supported by the presence of xenocrystic zircon of Mesoarchean age in gabbroic anorthosite (Rayner et al., 2011) from the Kokumiak River layered plutonic complex.

The presence of significant ortho- and clinoamphibole in some samples may reflect 1) partial hydration of pyroxenes through subsolidus reactions with water incorporated into the magma due to interaction with wall rocks; or 2) post-igneous metamorphism, known to have penetratively affected the region at 1860–1840 Ma (Berman et al., 2011).

GEOCHEMISTRY

Petrochemical Analyses

Whole-rock analyses of four samples with less than 50% SiO_2 are presented in Table 5. One of the analyzed samples is M38B-02, a two-pyroxene peridotite from the Kokumiak River layered plutonic complex. Given the probable interaction with crustal rocks and resultant effect on incompatible trace-element contents in these rocks, which should be inherently very low in these rocks, it is suspected that whole-rock

Table 4. Average microprobe analyses of amphiboles and phlogopite.

Sample	A21	M135	A21	B13
n	2	4	4	4
Type	trem	trem	phlog	phlog
SiO_2	50.00	49.63	38.93	38.27
TiO_2	0.30	0.38	1.42	0.87
Al_2O_3	6.31	6.17	14.61	14.18
Cr_2O_3	1.24	0.30	1.83	0.62
V_2O_3	0.03	0.02	0.05	0.02
FeO	8.24	6.63	9.91	3.94
MnO	0.16	0.11	0.03	0.03
MgO	17.51	18.57	18.95	23.69
NiO	0.24	0.05	0.37	0.18
ZnO	0.03	0.01	0.05	0.01
CaO	12.00	13.04	0.00	0.01
Na_2O	1.06	1.36	0.07	0.55
K_2O	0.52	0.39	9.55	8.59
BaO	0.00	0.04	0.08	0.10
P_2O_5	0.06	0.01	0.07	0.05
F	0.46	0.20	0.83	0.72
Cl	0.04	0.04	0.08	0.26
Total	**98.20**	**96.94**	**96.90**	**92.08**

n = number of analyses
phlog = phlogopite,
term = clinoamphibole (dominantly tremolite molecule)

Table 5. Whole-rock analyses of three peridotites from the study area.

Sample	C033A-01	M150A-02	M038B-02
Type	pr	pr	pr
SIO_2	40.9	41.7	47.0
TIO_2	0.09	0.29	0.26
Al_2O_3	0.6	5.4	1.5
Fe_2O_3	12.1	10.7	12.1
MnO	0.16	0.15	0.20
MgO	43.51	32.15	26.06
CaO	0.92	4.13	11.87
Na_2O	bd	0.3	bd
K_2O	0.01	0.14	0.02
P_2O_5	0.01	0.02	0.01
CO_2	0.2	0.2	0.4
sum	98.5	95.2	99.4
RB	0.1	1.9	1.2
Cs	bd	0.03	0.06
BE	1.0	bd	bd
SR	22	50	27
BA	17	3	17
Sc	10.0	16.4	28.9
Y	1.4	4.8	4.1
ZR	5	20	9
Hf	0.1	0.5	0.3
V	52	125	99
NB	0.2	0.4	0.3
Ta	0.1	0.1	0.1
CR	5043	18063	3200
Mo	bd	2.3	0.7
NI	209	161	116
CU	bd	25	bd
Ag	0.3	0.5	bd
ZN	69	73	91
Ga	1.1	5.3	2.8
Tl	bd	0.02	bd
Sn	bd	1.1	bd
La	0.32	2.00	0.91
Ce	0.74	4.10	2.40
Pr	0.10	0.49	0.38
Nd	0.42	2.10	2.00
Sm	0.14	0.51	0.67
Eu	bd	0.18	0.22
Gd	0.19	0.65	0.85
Tb	0.03	0.12	0.14
Dy	0.25	0.86	0.83
Ho	0.05	0.18	0.17
Er	0.17	0.57	0.45
Tm	0.03	0.08	0.06
Yb	0.22	0.56	0.39
Lu	0.04	0.09	0.06
Th	0.12	0.37	0.10
U	0.04	0.22	0.06
Pb	bd	2.0	1.0

All sample numbers prefixed by 07CYA-
Major elements (above sum) in weight %; trace elements in ppm
Analysis techniques and errors as per Whalen et al., 2010
bd = below detection level

Table 6. Selected assay data.

	Limit	Method	C33a2	Y110	M37b2	M38a1	B140a	S153a1	S153a2	Q27a1	Y123	M150a3	S145	Y117	T154	B140b
Ti,%	0.01	TD-ICP	0.02	0.02	0.11	0.13	0.12	0.07	0.07	0.09	0.10	0.09	0.15	0.16	0.21	0.15
Fe,%	0.01	INAA	6.76	4.43	8.99	8.31	6.48	6.87	6.82	6.25	6.89	6.62	6.76	9.63	9.93	3.83
Mn,%	1	ICP	0.12	0.10	0.17	0.15	0.13	0.11	0.11	0.11	0.11	0.11	0.16	0.16	0.21	0.06
Mg,%	0.01	ICP	23.00	22.40	19.30	17.90	17.10	16.20	16.10	15.60	15.50	15.00	13.10	12.40	8.98	2.07
S,%	0.01	ICP	bd	0.01	0.03	0.04	0.02	bd	bd	bd	0.03	0.02	0.04	0.02	0.23	bd
Sc,ppm	0.1	INAA	6.8	4	14.4	10	12.8	11.3	10.7	11.5	13.5	15.3	22.7	24.5	37.2	14.7
V,ppm	2	ICP	44	11	78	89	96	65	59	72	76	85	120	120	159	87
Cr,ppm	2	INAA	6590	1030	4640	1680	4760	5800	5660	4880	5220	9100	2310	2060	1500	70
Co,ppm	1	INAA	141	87	139	115	96	118	110	105	107	106	83	105	76	22
Ni,ppm	1	INAA	1930	2340	1710	1910	1450	1540	1510	1430	1330	1430	928	695	206	100
Pd,ppb	0.5	FAMS	3.4	bd	7	3	20	14	15	16	15	11	3	13	33	11
Pt,ppb	0.5	FAMS	0.9	bd	6	6	7	5	3	4	4	7	4	7	6	17
Cu,ppm	1	ICP	2	2	19	259	13	5	bd	37	15	40	29	35	596	24
Ag,ppm	0.3	INAA	bd	bd	bd	0.5	bd	bd	bd	bd	bd	bd	bd	bd	bd	bd
Au,ppb	1	FAMS	1	bd	12	13	3	bd	bd	69	bd	7	bd	5	6	7
Zn,ppm	1	INAA	59	85	93	70	61	52	48	49	56	42	87	74	104	33
Pb,ppm	3	ICP	10	5	5	6	bd	bd	bd	9	5	bd	6	bd	bd	8
As,ppm	0.5	INAA	bd	bd	1.9	bd	bd	bd	bd	bd	1.4	bd	12.3	bd	0.8	2.4
Sb,ppm	0.1	INAA	bd	bd	bd	bd	bd	bd	bd	bd	bd	bd	bd	bd	0.3	0.3

All samples have prefix 07CYA-
bd = below detection limit
Analysis methods: INAA = induced neutron activation; ICP = inductive coupled plasma spectrometry; FAMS = flame absorption spectrometry

analyses cannot confidently be used to classify or interpret the type of magma which produced the intrusions. Evidence for extensive crustal interaction includes a significant population of inherited Paleoproterozoic and Archean zircons in 1870 ± 10 Ma gabbroic anorthosite (sample 07CYA-M38; Rayner et al., 2011); the presence of primary phlogopite in some peridotites; and subsolidus hydration of olivine and pyroxene in most samples. The most pristine peridotite with LREE contents significantly above detection limits (sample 07CYA-M150A) was analyzed for Sm-Nd isotopic ratios (Whalen et al., 2011). Its $\varepsilon_{Nd,1.9\ Ga}$ of –6.8 is a clear indication that this sample also has been crustally contaminated.

Economic Assays

Selected assay data for samples with 9% Mg (15% MgO) or higher is in Table 6 (locations in Figure 1a). For rocks with more than 500 ppm Cr, Ni is strongly correlated with Mg and Cr, presumably due to incorporation in olivine and Mg-rich pyroxene, and to co-precipitation of chromite and high-Mg silicate phases. Platinum (average 5 ppb) and Pd (average 13 ppb) are not correlated with any other element, and are therefore probably not incorporated in any of the major phases observed. At this time, we cannot associate the PGEs with any mineral phase.

The exception may be sample B140b, which is included in Table 6 although it contains only 2.1% Mg. This sample was collected from a diorite/gabbro phase of one of the ultramafic bodies, near where it was intruded by a 2 m wide dyke of younger granite. This sample contains anomalous quantities of Pt (17 ppb). Elevated Pd (11 ppb), As (2.4 ppm), and Sb (0.3 ppm) may reflect Pt and Pd remobilization and localization by hydrothermal fluids.

REGIONAL SIGNIFICANCE OF SOUTHAMPTON ISLAND'S ULTRAMAFIC-MAFIC PLUTONIC ROCKS

Widespread, isolated exposures of ultramafic and mafic plutonic rocks are a notable feature of the Precambrian basement terrain of Southampton Island, Nunavut. Although the scale of our mapping does not allow correlations between exposures, understanding is emerging of at least three, apparently distinct, Paleoproterozoic ultramafic-mafic magmatic events affecting this region. Current lithological, structural, and isotopic data from Southampton Island, namely the presence of polydeformed ca. 2.77–2.76 Ga orthogneiss intruded by ca. 2.6 Ga granite (Rayner et al., unpub. data, 2009) with Nd model ages typically in the range of 3.0 to 3.5 Ga (Whalen et al., 2011), support its crustal affinity to the Archean Rae Craton. As such, ultramafic-mafic magmatism at ca. 2.05 Ga and 1.88–187 Ga on Southampton Island may reflect mid-crustal extension of Rae crust related to the opening and closing, respectively, of the ocean (Manikewan) separating the Rae and Superior cratons. Younger mafic (quartz dioritic) magmatism at ca. 1.84 Ga recorded on the eastern shore of Southampton Island (Rayner et al., 2011) may represent the western extension of the Cumberland Batholith, a 1.86–1.84 Ga post-accretion batholith (Whalen et al., 2010) interpreted to have stitched the terrane boundary between the Rae Craton and Meta Incognita (St Onge et al., 2000), a microcontinent exposed east of Southampton Island on southern Baffin Island (St Onge et al., 2006; Sanborn-Barrie et al., 2008b; St-Onge et al., 2009).

Correlations with other mafic igneous events in the region remain speculative. An isolated peridotite intrusion, similar to the Kokumiak River layered plutonic complex, emplaced into Paleoproterozoic granite is exposed near the west shore of central Baffin Island, north of Flint Lake (St-Onge et al., 2005). The central Baffin ultramafic complex is surrounded by a metre-thick rind of phlogopite. This intrusion may be related to the ca. 1.93 Ga Bravo Lake Formation which consists of mafic submarine flows and ultramafic-mafic sills (Johns et al., 2006), or may represent a younger magmatic event, possibly an expression of the 1.88–1.87 Ga mafic plutonic event now recognized on Southampton Island. It is difficult to compare the Bravo Lake Formation with the Kokumiak River layered plutonic complex on the basis of mineralogy, given that the Bravo Lake Formation is reported to have undergone hydrothermal alteration and prograde/retrograde metamorphism as a result of its proximity to the younger Cumberland batholith. Whole-rock analyses indicate that the Bravo Lake Formation, though dominated by mildly alkaline basalts, contains some tholeiitic compositions at high stratigraphic levels.

Mafic-ultramafic rocks exposed on Southampton Island both predate and postdate the ca. 1850 Ma Hudson granitoid suite (van Breemen et al., 2005) which extends from northern Saskatchewan to Greenland. The ca. 1850 Ma Hudson suite has no known mafic igneous trigger and, as such, had been interpreted as a product of in situ melting due to crustal thickening and subsequent extension (Peterson et al., 2002). However, some Hudson suite plutons immediately west of Southampton Island, in the area of Chesterfield Inlet, have young Nd model ages (ca. 2.4 Ga; Peterson et al., 2010), suggestive of a juvenile mantle component (Peterson and van Breemen, 1999). Also within the Chesterfield Inlet area, Sandeman et al. (2000) have described comingling between Hudson granitic melts and spessartite lamprophyre of broadly basaltic composition. The ultramafic-mafic plutonic phases of Southampton Island may be in the correct position, in time and space, to be implicated as, or related to, this 'missing' juvenile igneous event.

ACKNOWLEDGMENTS

The Southampton Island Integrated Geoscience project was funded by the Canada-Nunavut Geoscience Office through a Strategic Investments in Northern Economic Development (SINED) initiative and by the Geological Survey of Canada's Northern Mineral Resources and Development (NMRD) program. Logistical support was coordinated by Natural Resources Canada's Polar Continental Shelf Program. Mapping and sample collection by Julie Brown. Tim Bachiu and Donald James contributed to our understanding of Southampton's ultramafic plutonic rock suite. Patricia Hunt (SEM) and Katherine Venance (microprobe) provided invaluable technical assistance and expertise. A constructive review of this paper was provided by Joe Whalen.

REFERENCES

Berman, R.G., Rayner, N., Sanborn-Barrie, M., and Chakungal, J., 2011. New constraints on the tectonothermal history of Southampton Island, Nunavut, provided by in situ SHRIMP geochronology and thermobarometry; Geological Survey of Canada, Current Research 2011-6, 14 p. doi:10.4095/287287

Chakungal, J., Sanborn-Barrie, M., and James, D., 2007. Southampton Island: an updated geosciences database; 35th Annual Yellowknife Geoscience Forum, Abstracts Volume 2007.

Johns, S.M., Helmstaedt, H.H., and Kyser, T.K., 2006. Paleoproterozoic submarine intrabasinal rifting, Baffin Island, Nunavut, Canada: volcanic structure and geochemistry of the Bravo Lake Formation; Canadian Journal of Earth Sciences, v. 43, p. 593–616. doi:10.1139/e06-009

Peterson, T.D. and van Breemen, O., 1999. Review and progress report of Proterozoic granitoid rocks of the western Churchill Province, Northwest territories (Nunavut); *in* Current Research 1999-C, Geological Survey of Canada, p. 119–127.

Peterson, T.D., van Breemen, O., and Sandeman, H.A., 2002. Proterozoic (1.85–1.75 Ga) igneous suites of the western Churchill Province: granitoid and ultrapotassic magmatism in a reworked Archean hinterland; Precambrian Research, v. 119, p. 73–100. doi:10.1016/S0301-9268(02)00118-3

Peterson, T.D., Pehrsson, S., Skulski, T., and Sandeman, H., 2010. Compilation of Sm-Nd Isotope Analyses of Igneous Suites, Western Churchill Province; Geological Survey of Canada, Open File 6439, 1 CD-ROM. doi:10.4095/285360

Rayner, N., Chakungal, J., and Sanborn-Barrie, M., 2011. New U-Pb geochronological results from plutonic and sedimentary rocks of Southampton Island, Nunavut; Geological Survey of Canada, Current Research 2011-5, 20 p. doi:10.4095/287286

Ross, M. and Kosar, K., 2009. Geochemical and indicator mineral reconnaissance survey of surficial sediments, Southampton Island, Nunavut; Geological Survey of Canada, Open File 6078, 76 p. doi:10.4095/247643

Sanborn-Barrie, M., Chakungal, J., James, D., Whalen, J., Zhang, S., Ross, M., Berman, R., Rayner, N., and Gilbert, C., 2008a. A new understanding of the geology of Southampton Island, Nunavut, in a NE Laurentia Context; Poster Presentation at Mineral Exploration Roundup, Vancouver, British Columbia, January 2008.

Sanborn-Barrie, M., St-Onge, M.R., Young, M.D., and James, D.T., 2008b. Bedrock geology of southwestern Baffin Island, Nunavut: Expanding the tectonostratigraphic framework with relevance to mineral resources; Geological Survey of Canada, Current Research 2008-6, 16p. doi:10.4095/225179

Sandeman, H.A., LePage, L.D., Ryan, J.J., and Tella, S., 2000. Field evidence for commingling between ca. 1830 Ma lamprophyric, monzonitic and monzogranitic magmas, MacQuoid-Gibson Lakes area, Kivalliq Region, Nunavut; Current Research 2000-C5, Geological Survey of Canada, 10 p. doi:10.4095/211099

St-Onge, M.R., Scott, D.J., and Lucas, S.B., 2000. Early partitioning of Quebec: Microcontinent formation in the Paleoproterozoic; Geology, v. 28, p. 323–326. doi:10.1130/0091-7613(2000)28<323:EPOQMF>2.0.CO;2

St-Onge, M.R., Scott, D.J., and Wodicka, N., 2005 Geology, Ikpik Bay, Baffin Island, Nunavut; Geological Survey of Canada, Map 2077A, scale 1:100 000.

St-Onge, M.R., Searle, M., and Wodicka, N., 2006. Trans-Hudson Orogen of North America and Himalayan-Tibetan Orogen of Asia: Structural and thermal characteristics of the lower and upper plates; Tectonics, v. 25, cit. no. TC4006. doi:10.1029/2005TC001907.

St-Onge, M.R., Van Gool, J.A.M., Garde, A.A., and Scott, D.J., 2009, Correlation of Archaean and Palaeoproterozoic units between northeastern Canada and western Greenland: constraining the pre-collisional upper plate accretionary history of the Trans-Hudson Orogen; *in* Earth Accretionary Systems in Space and Time, (ed.) P.A. Cawood and A. Kroner; Geological Society, London, Special Publication 318, p. 193–235.

van Breemen, O., Peterson, T.D., and Sandeman, H.A., 2005. U-Pb zircon geochronology and Nd isotope geochemistry of Proterozoic granitoids in the western Churchill Province: intrusive age pattern and Archean source domains; Canadian Journal of Earth Sciences, v. 42, p. 339–377. doi:10.1139/e05-007

Whalen, J.B., Wodicka, N., Taylor, B.E., and Jackson, G.D., 2010. Cumberland Batholith, Trans-Hudson Orogen, Canada: Petrogenesis and implications for Paleoproterozoic crustal and orogenic processes; Lithos, v. 117, p. 99–118. doi:10.1016/j.lithos.2010.02.008

Whalen, J.B., Sanborn-Barrie, M., and Chakungal, J., 2011. Geochemical and Nd isotopic constraints from plutonic rocks on the magmatic and crustal evolution of Southampton Island, Nunavut; Geological Survey of Canada, Current Research 2011-2, 11 p. doi:10.4095/286319

Geological Survey of Canada Project MGM007